IRAQI Academic Scientific Journals

Samarra Journal of Pure and Applied Science

SJPAS

www.sjpas.com

p ISSN: 2663-7405
e ISSN: 2789-6838

# Synthesis and characterization of thermochemical spray nickel oxide- cobalt oxide Nano composite As a $CO_2$ gas sensor

**Mohammed Najeeb. Jasim*, Eid Mohammed Monawer**

Department of General sciences, College of Basic Education\Haditha, University of Anbar, Iraq



https://doi.org/10.54153/sjpas.2025.v7i2.962

**Article Information**

Received: 10/07/2024
Revised: 17/08/2024
Accepted: 15/09/2024
Published: 30/06/2025

**Keywords:**

NiO, $Co_3O_4$, $CO_2$, thin films, Gas Sensor.

**Corresponding Author**

E-mail: mhamad87@uoanbar.edu.iq
Mobile:

**Abstract**

In this research, cobalt oxide's pure nano thin films of were prepared, and a mixture of cobalt oxide ($Co_3O_4$) and nickel oxide (NiO) was prepared in volumetric proportions of nickel oxide that included (10,20vol%) by thermal chemical spraying method, deposited on bases of glass at a temperature of (250 °C). The results of X-ray examinations of the prepared membranes showed that they have a polycrystalline composition, and that the prepared membranes formed a nanocomposite of cobalt and nickel. The formula Debye Scherer was used to calculate the crystal size. The nanoscale was decreasing with increasing(10,20%) the mixing ratio of nickel oxide for membranes deposited on glass bases Dimensions (2×2cm) , decreasing from (19.6 nm) for pure cobalt oxide to (8.45875 nm). Cobalt oxide mixed with 20% nickel. Use an atomic force microscope (AFM) to determine the grain size, roughness rate, and square root square mean, The images showed that the surface of the membranes is homogeneous, and that the average granular size of all membranes is nano-size and its value changes with the change of mixing ratio, the optical transmittance of the prepared membranes was calculated, using a spectrophotometer and the wavelength ranges between, (nm1100-nm3000). It was found that the increase in the mixing ratio leads to a decrease in the transmittance, while the optical energy gap also decreased with the increase in the mixing ratio. The results confirmed that the cobalt oxide membranes inlaid with nickel oxide have a high degree of sensitivity towards $CO_2$ gas, as the sensitivity values depend on the mixing ratios, base temperature and gas concentration. It was found that the relative sensitivity values (S%) for $Co_3O_4$ – NiO) ,thin films deposited on glass bases towards ($Co_2$) gas, have a sensitivity value of up to (70.7) at the highest concentration (242ppm) and at a temperature of (100C°), as sensitivity increases with increasing gas concentration. The study also proved that nanothinfilms mixed of $Co_3O_4$-NiO prepared by thermal chemical decomposition method give gas sensors with good properties towards $CO_2$ even at room temperature.

**Introduction:**

Nanomaterials are of particular importance due to their unique range of properties, including magnetic, insulating, thermal, optical, and catalytic characteristics. There is an increasing trend towards developing composite materials that incorporate multiple nanomaterials to enhance overall properties. This trend is driven by the observation that nanomaterials often exhibit unexpected traits, opening up new opportunities for applications in various fields, including nanomedicine [1,2]. Transition metal oxides, such as nickel oxide, iron oxide, and cobalt oxide nanoparticles, are notable for their excellent durability and electrochemical stability. Among these oxides, nickel oxide (NiO) and cobalt oxide (Co3O4) have garnered significant attention due to their applications in various technological fields when reduced to nanoscale systems [4-7]. Co3O4 and NiO are widely studied transition metal oxides with desirable properties. Their nanostructured forms often exhibit unique characteristics compared to their bulk counterparts, primarily due to surface effects and particle size. Both $Co_3O_4$ and NiO are p-type semiconductors with band gaps in the range of 3.4-4 eV [9]. These oxides are low-cost, stable, and environmentally friendly [10-14]. However, their low conductivity is a limitation. Nevertheless, their electrochemical properties can be improved by combining these metal oxides, as mixed metal oxides exhibit enhanced oxidation and reduction behaviors compared to their individual counterparts [16-18]. These oxides have significant potential in fields such as magnetic devices, battery cathodes, and gas sensors [19]. Magnetic nanomaterials are used in sensors, MRI, data storage, and medical applications [20]. Semiconductor oxides have been extensively studied for gas sensing applications due to their sensitivity to many toxic and polluting gases. The conductivity of these oxides changes significantly upon exposure to gases. Efforts have been made to enhance the performance of gas sensors by improving sensitivity, extending sensor life, reducing response and recovery times, and lowering operating temperatures [21]. Additionally, research has focused on using mixtures of metal oxides to improve sensitivity and selectivity. The interaction processes between gases and semiconductor metal oxides involve two types: interaction with the oxide surface and interaction within the oxide, which alters the sensor's electrical resistance [22]. Semiconductor gas sensors, including those based on $SnO_2$, $In_2O_3$, ZnO, $WO_3$, and $TiO_2$, offer advantages such as small size, high sensitivity, and low cost. Their performance is influenced by grain boundary effects, driving research towards nanometer-sized materials [23,24]. Carbon dioxide ($CO_2$) is a gas with notable effects on human health, with concentrations ranging from 350 to 800 ppm in natural conditions. In poorly ventilated indoor environments, $CO_2$ levels can exceed 1000 ppm, leading to health issues such as fatigue, headaches, and respiratory problems. Therefore, detecting $CO_2$ concentrations is vital for maintaining healthy environments. Various gas sensing technologies, including optical, semiconductor, and electrochemical methods, have been developed to detect $CO_2$. However, these sensors often suffer from high power consumption, high operating temperatures, and long detection times [25]. To address these issues, researchers have explored the sensitivity of different materials to CO2. For example, Ogura studied $CO_2$ sensors based on polymeric compounds such as Emerald base poly aniline (EB-PAn) and polycarbonate (PVA), achieving a sensitivity of 25% with optimized ratios [26]. Alwan also studied the response of gold films on porous silicon to $CO_2$, reporting a maximum sensitivity of 72% [27]. This research aims to develop highly sensitive $CO_2$ sensors using nanofilms.

**Experimental details**

Cobalt oxide and nickel oxide films ($CO_3O_4$:NiO) are deposited in proportions (NiO10, 90 $CO_3O_4$,) on glass substrates using CSP technology at (300 °C). Two different solutions were prepared with a concentration of (0.1M) using cobalt chloride prepared by SCHUCHARRAD with purity of 99.9%, and a molecular weight of (273.93Mw=). (2.73g) was dissolved in (100ml) of distilled water and nickel chloride using aqueous nickel chloride (NiCl2.6H2O) processed with purity of 99.9%, and its molecular weight (Mw=237.69), mol/L). (.372 g) was dissolved in (100ml) of distilled water and then the solution is mixed with a magnetic stirrer for an hour at a temperature of 40 °C, Thus, we get a solution of cobalt chloride and nickel, which is a clear transparent solution, and left for 24 hours, to ensure that there is no sediment or stuck, and to be sure of the homogeneity of the solution Watch it with your eyes, there are no plankton or impurities after spraying. The formation of the NiO membrane on the hot base is represented by the following equations. [28,29]

$$3CoCl_2.2H_2O+2H_2O \longrightarrow Co_3O_4+4H_2Cl + Cl_2 \ldots..(1)$$

$$3NiCl_2.2H_2O+H_2O \longrightarrow 3NiO+2H_3Cl + 2Cl_2 \ldots(2)$$

The spray nozzle is (25 cm) away from the substrates at a spray rate (2 ml/min). The composition of thin films ($CO_3O_4$) is described by the equation [28, 29], various techniques were used for examination. The structural properties of the membranes were examined using (XRD-6000 X-ray(Cu Kα radiation, λ=0.154 nm) in 2θ range from 20° to 70) with an X-ray source using Cu K radiation with a wavelength of (1.54056), within the range (20-80°). AFM modelling was used to characterize the surface formation of Thin films(SPM-AA3000). The Optical properties were determined by using UV–VIS OPTIMA SP-3000 Wavelength Range1100-190

**Results and Discussion**

**XRD Analysis**

figure (1) at the bottom shows XRD patterns of cobalt oxide thin **films The results of X-ray** diffraction examination of Co3O4 films deposited on glass bases at a temperature of (250 °C) showed that they are polycrystalline with peaks (400), (220), (111), (311), (422), (440), (220) as shown in Figure (3-1-a), and the preferred direction (220) at (.54322Θ=) which has a hexagonal structure and this corresponds to the card (1049-047 JCPDS), and agrees with what The researcher (M. S. Jamal) and his group found [30]. The crystal volume was calculated using the equation of (Sheerer) [31] as in the following equation: $D = \frac{K\lambda}{\beta \times COS\theta}$.....(3)

Whereas:

D : grain size (nm), : θ diffraction angle, : K constant value (0.9).

: λThe wavelength of the X-rays used is equal to 4A (1.5°).

: βdisplay value at the middle of the highest value (FWHM).

figure (1-3 -b) shows the increase in the intensity of the peaks of CoO and the decrease of other peaks, and that the average crystal size has decreased to (15.879 nm). Figure (c-1-3) shows at a mixing ratio (20% of NiO -80% Co3O4), the decrease in the peak strength of the NiO compound, which means a decrease in crystallization due to mixing with Co3O4, and the presence of seven peaks (113), (440), (422), (111), (311), (220), (101) and the preferred direction (022) at (2Θ=32.4109), which has a cubic structure and this corresponds to the card (01-080-1532) and agrees with the researcher 32](X. W. Wang)] and that its average crystal size is (8.45875 nm).

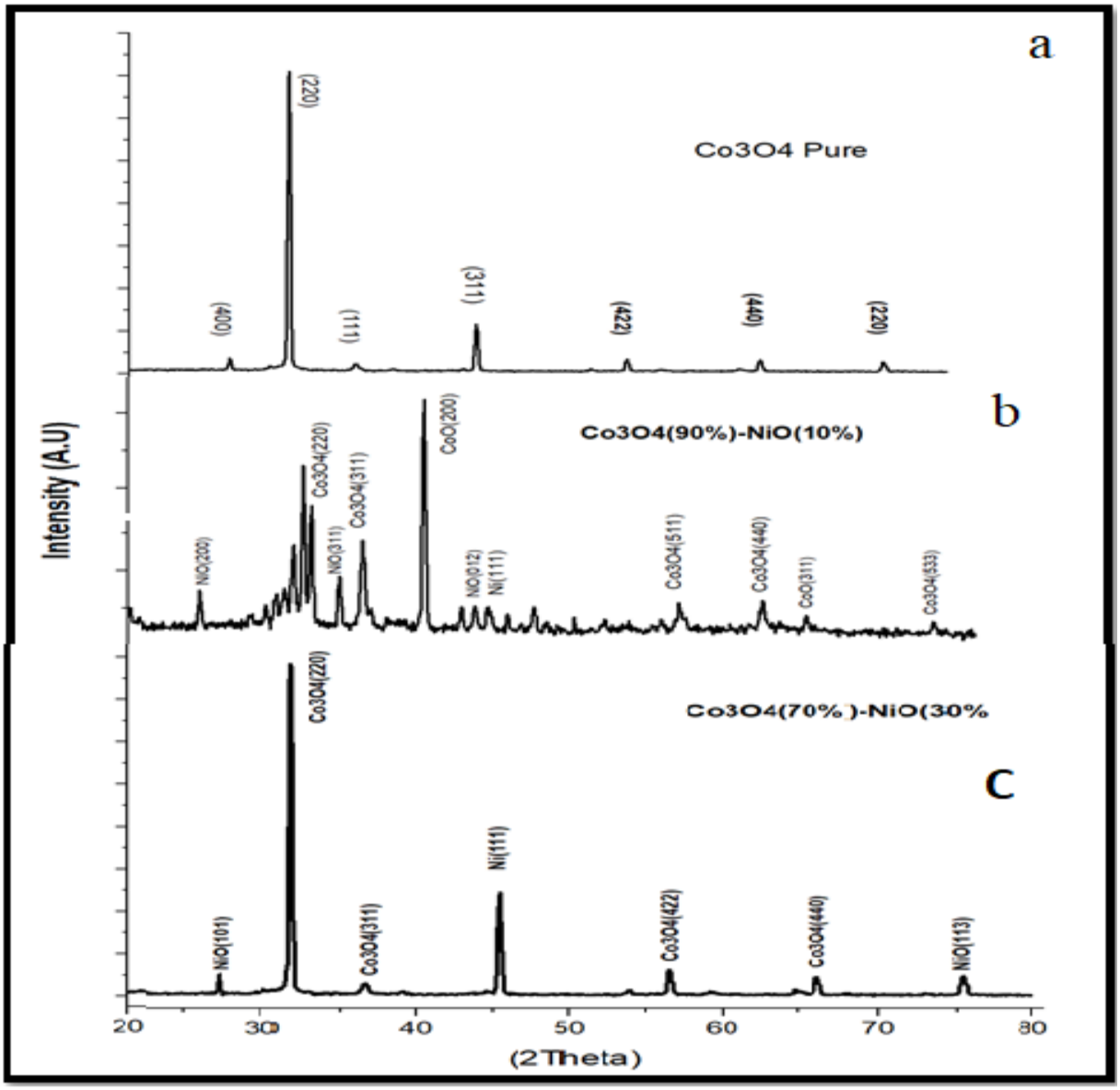


**Fig. 3-1** *shows the X-ray diffraction of Co3O4 (Co3O4-NiO) films deposited on glass*

**Table (3-1)** shows the values of diffraction angles for intensity, d hkl and grain size of (Co3O4-NiO) films deposited on glass

| Sample | Phase | Hkl | 2theta (Exp.) | dhkl Exp.(Å) | dhkl Std.(Å) | FWHM | G.S (nm) |
|---|---|---|---|---|---|---|---|
| A | $Co_3O_4$ | 111 | 19.001 | 4.6670 | 4.6448 | 0.295 | 5.95 |
| | $Co_3O_4$ | 220 | 31.272 | 2.8580 | 2.8183 | 0.246 | 4.95 |
| | $Co_3O_4$ | 311 | 36.576 | 2.4370 | 2.4567 | 0.295 | 11.32 |
| | $Co_3O_4$ | 400 | 45.505 | 2.0210 | 1.9933 | 0.295 | 102. |
| | $Co_3O_4$ | 422 | 56.448 | 1.6501 | 1.6301 | 0.2952 | 4.92 |
| | $Co_3O_4$ | 440 | 66.195 | 1.4118 | 1.4290 | 0.344 | 4.30 |
| | CoO | 220 | 75.306 | 1.2609 | 1.2532 | 0.360 | 4.03 |
| B | Co3 O4 | 111 | 19.001 | 4.4109 | 4.6670 | 0.147 | 9.92 |
| | $Co_3O_4$ | 220 | 31.061 | 2.8792 | 2.8580 | 0.393 | 3.92 |
| | $Co_3O_4$ | 311 | 36.673 | 2.4505 | 2.4370 | 0.344 | 8.10 |
| | CoO | 200 | 40.900 | 2.3501 | 2.2720 | 0.246 | 5.89 |
| | NiO | 012 | 43.602 | 2.0758 | 2.0884 | 0.196 | 7.91 |
| | Ni | 111 | 44.471 | 2.0210 | 2.0372 | 0.246 | 6.66 |
| | $Co_3O_4$ | 422 | 55.278 | 1.6501 | 42.6600 | 0.787 | 6.21 |
| | CoO | 200 | 57.106 | 1.6129 | 1.6065 | 0.246 | 6.93 |
| | $Co_3O_4$ | 511 | 58.988 | 1.5658 | 1.5557 | 0.196 | 9.63 |
| | $Co_3O_4$ | 440 | 64.950 | 1.4358 | 1.4290 | 0.147 | 18.83 |

| | | | | | | | |
|---|---|---|---|---|---|---|---|
| | | | | | | | |
| | **CoO** | **311** | **67.979** | **1.3790** | **1.3700** | **0.196** | **17.43** |
| | **$Co_3O_4$** | **533** | **77.020** | **1.2752** | **1.2328** | **0.147** | **89.12** |
| **C** | **$Co_3O_4$** | **220** | **31.635** | **2.8283** | **2.8580** | **0.196** | **7.53** |
| | **$Co_3O_4$** | **311** | **36.624** | **2.4537** | **2.4370** | **0.147** | **20.61** |
| | **Ni** | **111** | **44.633** | **2.0302** | **2.0340** | **0.147** | **12.32** |
| | **Co3O4** | **422** | **56.460** | **1.6298** | **1.6501** | **0.295** | **4.92** |
| | **Co3O4** | **1.55570** | **59.244** | **1.5597 ** | **1.5557** | **0.492** | **5.95** |
| | **$Co_3O_4$** | **440** | **64.816** | **1.43846** | **1.4290** | **0.147** | **4.95** |
| | **$Co_3O_4$** | **440** | **66.212** | **1.4114** | **1.4290** | **0.246** | **6.56** |
| | **NiO** | **113** | **75.352** | **1.2603** | **1.2595** | **0.301** | **4.83** |

**Atomic Force Microscopic (AFM)**

Atomic force microscopy (AFM) is used to study surface roughness and to know the granular size, and it is one of the microscopes with high analytical ability, as it gives an image of the surface whose magnification capacity exceeds 1000 times the optical diffraction microscopes. Figure (3-2) shows the atomic force microscope images of cobalt oxide membranes (Co3O4) mixed with nickel oxide (NiO) deposited on bases of glass, and shows the topography of the surface with high homogeneity and uniform granular distribution. Figure (2-3-a) shows the images of cobalt oxide in a pure way. While Figure (3-2-b) shows the images of cobalt oxide mixed with nickel oxide by (90% Co3O4-10%NiO). Figure (3-2-c) shows the images of cobalt oxide mixed with nickel oxide by (80% Co3O4-20% NiO). We notice from Figure (3-2-b) and Figure (3-2-c) that the greater the mixing ratio of nickel oxide, the greater the granular size and the reason is due to the granular size of cobalt oxide, which is larger than nickel oxide.

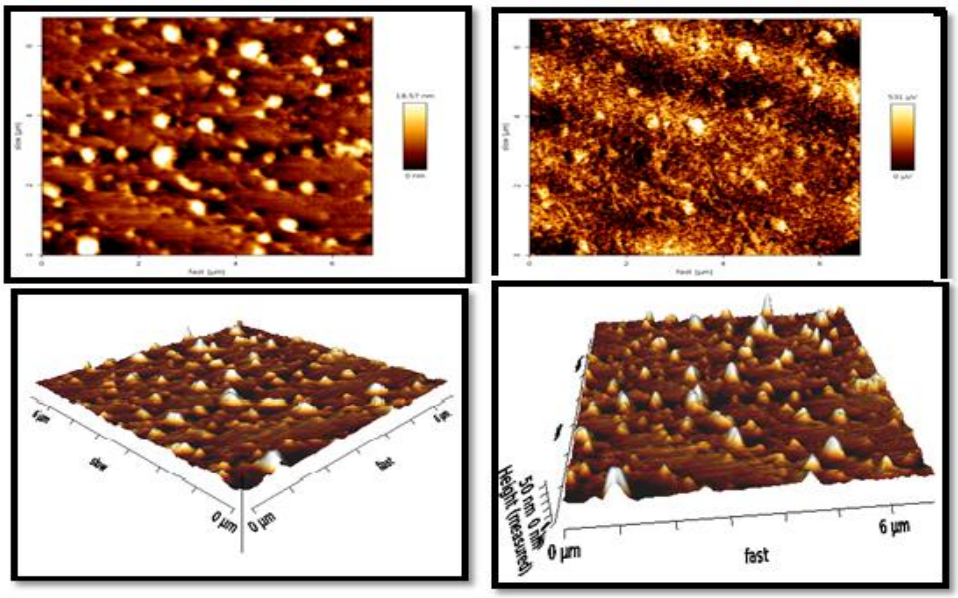


**Fig (a-2-3)** *shows AFM images of cobalt oxide*

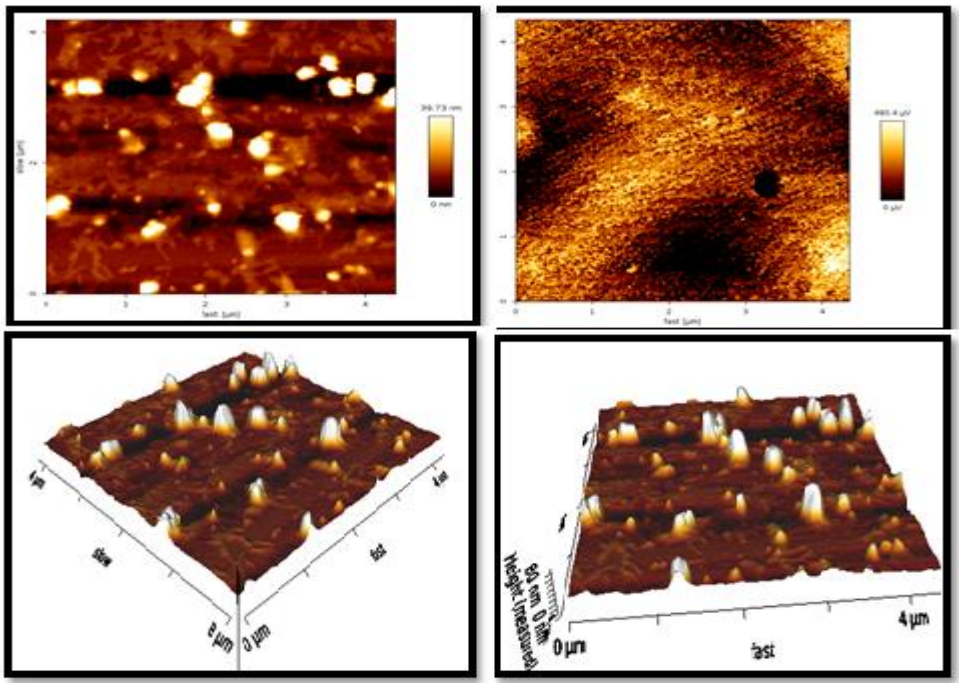


**Fig. (3-2-b)** *Pictures (AFM) (90% Co3O4 -10% NiO)*

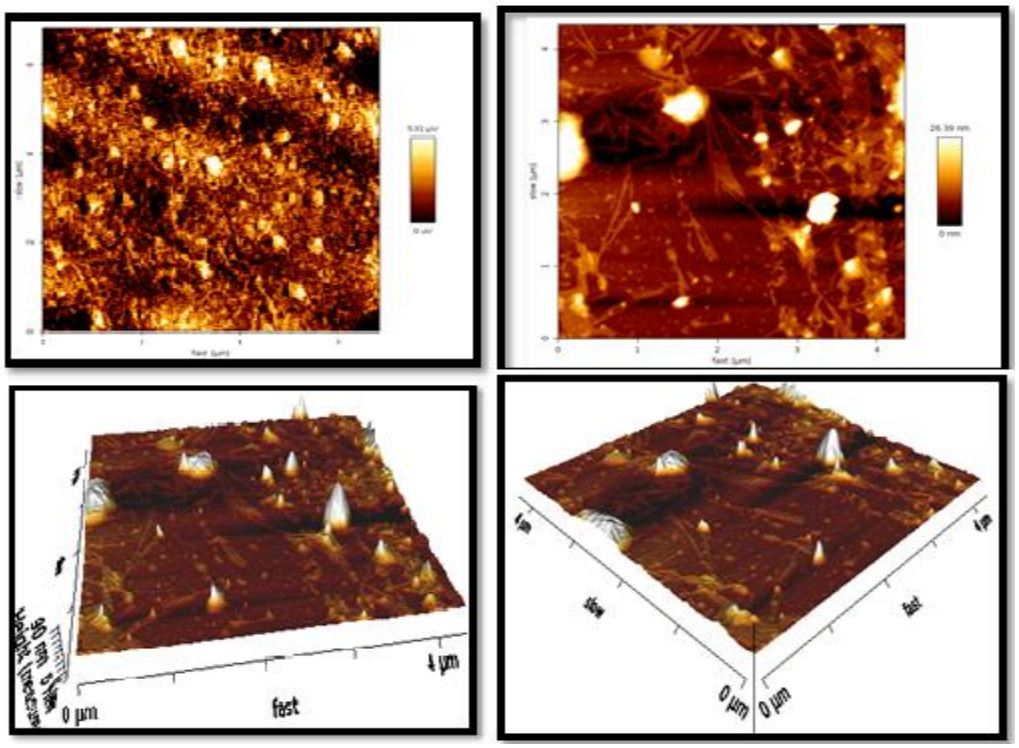


**Fig. (3-2-c)** *shows the AFM images of cobalt oxide with nickel oxide in a ratio of (80% $CO_3O_4$ - 20% NiO)*

## Optical measurement results

*Optical permeability of membranes*

Permeability is the ratio between the intensity of the transmitted ray (I_T) and the intensity of the incident ray (I_°). It is denoted by the symbol τ, which is a unit-free quantity and the permeability depends on the membrane thickness, the percentage of distortion and the temperature of the base[32]. Permeability can be calculated through the following equation:

$$\tau = \frac{I_T}{I_\circ} \ldots\ldots(4)$$

T is the transmittance, $I_T$ is the subtle light (or reading) that is experienced through matter, $I_\circ$ is the light (or reading) light on the material.

Measurements of permeability within the range (nm1080-nm180) were studied for each of the cobalt oxide and nickel oxide membranes prepared and deposited on glass in different proportions of the mixture (Co3O4-NiO) where the permeability of (Co3O4) membranes is high as its permeability reached 93% and this shows the curve a)) and when we started mixing by (Co3O4) 90% with NiO) (by 10%, which was its purity (87%) and this is shown by the indicator (b) and when we mixed with 20% of nickel oxide and 80% of cobalt oxide, the permeability was ( 66%) This is shown by the indicator (C), which causes an increase in the sedimentation time that leads to an increase in thickness. This increase in thickness causes surface roughness and increased scattering, which leads to a decrease in wavelength permeability when mixing. Where Figure (3-3) shows the permeability curves as the wavelength function, as we notice from the figure that the permeability of the membranes is large and then begins to decrease when the mixing ratios increase.

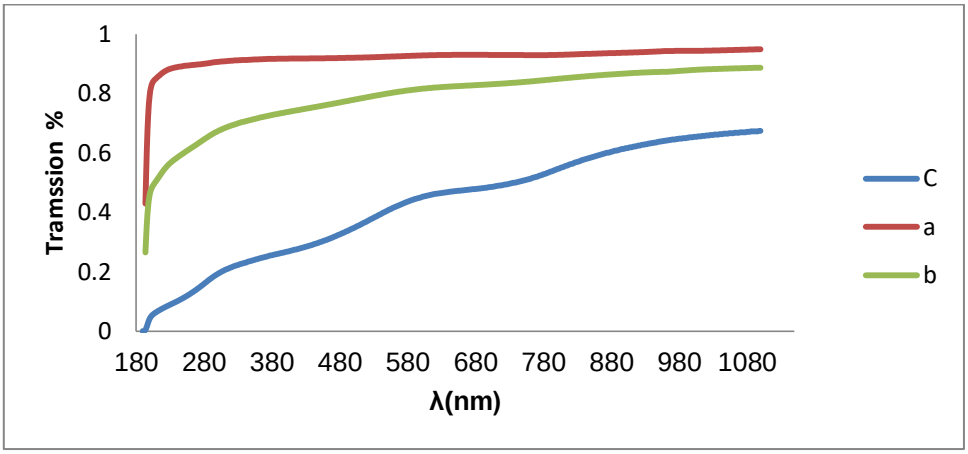


**Fig. (3-3)** *shows the permeability of ($CO_3O_4$-NiO) films deposited on glass*

**Table (3-2)** shows the permeability ratios of ($CO_3O_4$-NiO) membranes deposited on glass

| NO | | T% |
|---|---|---|
| A | CoO PURE | 93% |
| B | CoO90%- NiO10% | 87% |
| C | CoO80%- NiO20% | 66% |

*Optical energy gap. Optical Energy Gap*

The gap of the optical energy is of great significance in determining the capability of employing thin films in sensors application, because it exhibits a bright idea of optical absorption. This is due to the transparent property of membrane to radiation, whose energy is less than the energy gap (Eg>hv) and absorbent the radiation, whose energy is greater than it (Eg≤hv). The energy gap has been calculated in the permissible electronic transitions of CoO and NiO membranes, where we note from Figure (3-4) that the energy gap and the decrease in the gap that was deposited on Glass, as the optical energy gap of cobalt oxide was high and when mixing by 10% of nickel oxide, the energy gap decreased from 3.66 to 3.41 and continues to decrease with the increase in the mixing ratio to reach a mixing ratio of 20% to 3.3, and this means that the optical energy gap is large in the pure state and then begins to decrease when mixing and continues to decrease with the increase in the mixing ratio.

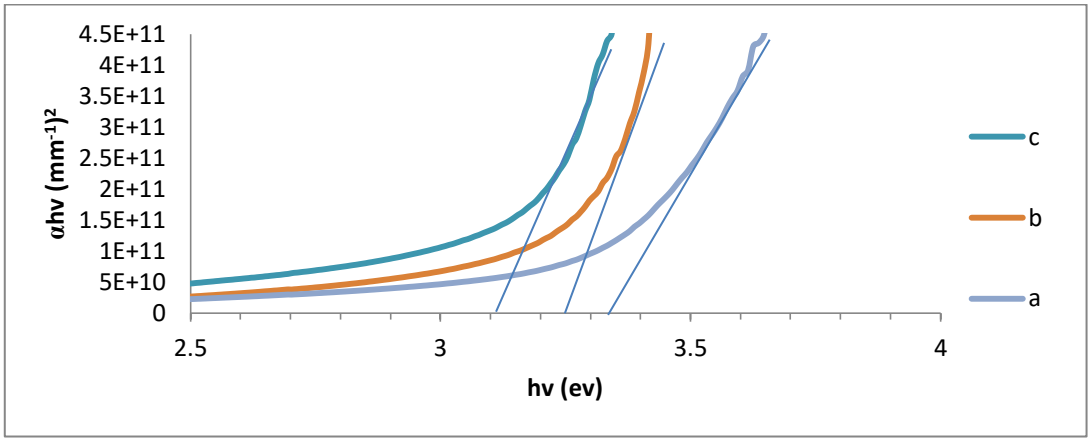


**Fig. (3-4)** *shows the energy gap of $CO_3O_4$-NiO films deposited on glass*

**Table (3-3)** shows the energy gap values of $CO_3O_4$-NiO membranes deposited on glass

| | sample | Energy gap(EV) |
|---|---|---|
| A | CoO PURE | 3.66 |
| B | CoO90%- NiO10% | 3.41 |
| C | CoO80%- NiO20% | 3.33 |

*$CO_2$ Gas Measurement of gas $CO_2$ sensor*

The sensitivity of metal oxides to gases depends on several factors, including temperature, type of material, crystal structure, grain size, surface topography, porosity and others, while temperature has a major role in the process of interaction of the gas with the surface of the sensor, as it occurs in a dynamic process dependent on temperature.

The air oxygen molecule can bind at the sites of the voids on the metal oxide surface, thus taking electrons from the surface of the oxide and turning into a negative ion, that results in an increase in the resistance of the surface, and the process of oxygen interaction with oxide can be represented by the following equations:[24]

$$O_2(gas) \rightleftharpoons O_2(ads) \quad \text{.....(5)}$$

$$O_2 + e^- \rightleftharpoons {}^-O_2(ads) \quad \text{.....(6)}$$

$$O_2(ads) + e^- \rightleftharpoons 2\,{}^-O(ads) \quad \text{.....(7)}$$

$$O^-(ads) + e^- \rightleftharpoons O^{-2}(ads) \quad \text{.....(8)}$$

When $CO_2$ gas is introduced on the metal oxide surface, there will be a reaction between the gas molecules and the adsorbed oxygen, as well as with the surface granules, and in this process $CO_2$ gas takes electrons from the oxide surface, thus increasing the resistance of the surface and the process continues until the saturation process occurs, and then the surface resistance stabilizes, from which the response time can be calculated and then the gas is discharged and the resistance begins to decrease until it reaches a value close to the starting point, as the time taken to be the recovery time is calculated.

The calculation of the relative sensitivity (S%) was based on the following equation:

$$S\ \% \ = \ \frac{Rg - Ra}{Rg} * 100\% \ldots . (9)$$

Figure (5-3) illustrates the change of relative sensitivity with the reaction time of $CO_2$ gas in different concentrations with the surface of the prepared membranes deposited on glass bases, from which response time (TRES), the highest sensitivity, and recovery time (trec) of different membranes can be calculated, at different temperatures.

Figure (3-5) clarifies that the sensitivity increases with the increase in the concentration of the gas when entering the $CO_2$ gas to reach the highest value and then stabilize and in the case of discharge of the gas, the sensitivity decreases to reach a value close to the starting point and not return to the starting point, due to the lack of extortion of all gas molecules. Table (3-4) shows the relative sensitivity values (S%) and the recovery time, and the response time of ($CO_3O_4$-NiO) films deposited on glass bases towards ($CO_2$) gas, it was found that the highest sensitivity value (70.7) at the concentration of (ppm242) and at a temperature of (100C°)

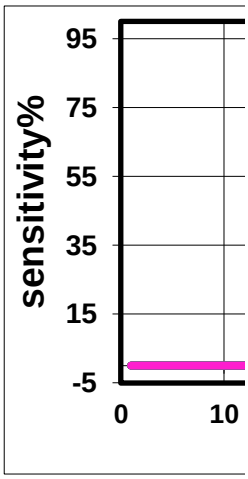


| Concet. | Sensitivity(%) | Res. T | Rec.T |
|---|---|---|---|
| 62 ppm- RT | 25.3 | 14.2 | 18.7 |
| 150ppm-RT | 40.1 | 14.2 | 18.2 |
| 242ppm-RT | 52.1 | 9 | 13.2 |
| 242ppm- 50 oC | 45.3 | 15.1 | 6.4 |
| 242ppm- 100 oC | 70.7 | 17.8 | 10.6 |

**Fig. (5-3)** *shows the change of sensitivity over time in the presence of $CO_2$ gas for the film ($CO_3O_4$-NiO) deposited on the bases of the glass for different concentrations of the ga*

**Table (3-4)** shows the values of sensitivity, response time and retrieval time

## Conclusions:

The results of this study demonstrate that nickel-cobalt mixed oxide nanoparticles can be easily prepared using the thermal chemical spraying technique. XRD analysis revealed that the crystal size of the nanoparticles decreases with an increasing proportion of nickel oxide (NiO) in the thin films. Optical property studies showed that the band gap decreases with an increase in nickel oxide content. Atomic force microscopy (AFM) indicated an average particle size of 93.5 nanometers, and surface roughness was found to increase with the mixing ratio, ranging from 14.2 nanometers. This increase in surface roughness enhances gas-surface interactions, leading to improved sensitivity to CO2 gas and better sensor performance.

**Acknowledgements**

*The authors would like to acknowledge the contribution of the University of Anbar (www.uoanbar.edu.iq) via their prestigious academic staff in supporting this research with all required technical and academic support.*

**References:**

[1] Makhlouf, S. A. (2002). Magnetic properties of Co3O4 nanoparticles. Journal of magnetism and magnetic materials, 246(1-2), 184-190.
[2] Arshad, Mohd, et al. "Effect of Co substitution on the structural and optical properties of ZnO nanoparticles synthesized by sol–gel route." Journal of alloys and Compounds 509.33 (2011): 8378-8381..
[3] Uflyand, I. E., & Dzhardimalieva, G. I. (2018). Nanomaterials preparation by thermolysis of metal chelates. Springer International Publishing..
[4] Sun, Q., & Bao, S. (2013). Effects of reaction temperature on microstructure and advanced pseudocapacitor properties of NiO prepared via simple precipitation method. Nano-Micro Letters, 5, 289-295.
[5] Morozov, Y. G., Ortega, D., Belousova, O. V., Parkin, I. P., & Kuznetsov, M. V. (2013). Some peculiarities in the magnetic behavior of aerosol generated NiO nanoparticles. Journal of Alloys and compounds, 572, 150-157.
[6] Zhang, H. T., Wu, G., Chen, X. H., & Qiu, X. G. (2006). Synthesis and magnetic properties of nickel nanocrystals. Materials Research Bulletin, 41(3), 495-501.
[7] Yang, Q., Sha, J., Ma, X., & Yang, D. (2005). Synthesis of NiO nanowires by a sol-gel process. Materials Letters, 59(14-15), 1967-1970.
[8] Huang, X., Wu, J., Guo, R., Lin, Y., & Zhang, P. (2014). Aligned nickel–cobalt oxide nanosheet arrays for lithium ion battery applications. International journal of hydrogen energy, 39(36), 21399-21404.
[9] El-Kemary, M., Nagy, N., & El-Mehasseb, I. (2013). Nickel oxide nanoparticles: synthesis and spectral studies of interactions with glucose. Materials Science in Semiconductor Processing, 16(6), 1747-1752.
[10] Anand, G. T., Nithiyavathi, R., Ramesh, R., Sundaram, S. J., & Kaviyarasu, K. (2020). Structural and optical properties of nickel oxide nanoparticles: Investigation of antimicrobial applications. Surfaces and Interfaces, 18, 100460.
[11Ramesh, R., Yamini, V., Sundaram, S. J., Khan, F. L. A., & Kaviyarasu, K. (2021). Investigation of structural and optical properties of NiO nanoparticles mediated by Plectranthus amboinicus leaf extract. Materials Today: Proceedings, 36, 268-272.
[12] Nakate, U. T., Patil, P., Choudhury, S. P., & Kale, S. N. (2018). Microwave assisted synthesis of Co3O4 and NiO nanoplates and structural, optical, magnetic characterizations. Nano-Structures & Nano-Objects, 14, 66-72.
[13] Murugesan, A., Loganathan, M., Kumar, P. S., & Vo, D. V. N. (2021). Cobalt and nickel oxides supported activated carbon as an effective photocatalysts for the degradation Methylene Blue dye from aquatic environment. Sustainable Chemistry and Pharmacy, 21, 100406.
[14] Din, M. I., Nabi, A. G., Rani, A., Aihetasham, A., & Mukhtar, M. (2018). Single step green synthesis of stable nickel and nickel oxide nanoparticles from Calotropis gigantea: catalytic and antimicrobial potentials. Environmental Nanotechnology, Monitoring & Management, 9, 29-36.

[15] Aravind, M., Ahmad, A., Ahmad, I., Amalanathan, M., Naseem, K., Mary, S. M. M., ... & Zuber, M. (2021). Critical green routing synthesis of silver NPs using jasmine flower extract for biological activities and photocatalytical degradation of methylene blue. Journal of Environmental Chemical Engineering, 9(1), 104877.
[16 ] Hou, J., Wang, Y., Zhou, J., Lu, Y., Liu, Y., & Lv, X. (2021). Photocatalytic degradation of methylene blue using a ZnO/TiO2 heterojunction nanomesh electrode. Surfaces and Interfaces, 22, 100889.
[17] Soto-Robles, C. A., Nava, O., Cornejo, L., Lugo-Medina, E., Vilchis-Nestor, A. R., Castro-Beltrán, A., & Luque, P. A. (2021). Biosynthesis, characterization and photocatalytic activity of ZnO nanoparticles using extracts of Justicia spicigera for the degradation of methylene blue. Journal of Molecular Structure, 1225, 129101.
[18] Nassar, M. Y., Aly, H. M., Abdelrahman, E. A., & Moustafa, M. E. (2017). Synthesis, characterization, and biological activity of some novel Schiff bases and their Co (II) and Ni (II) complexes: a new route for Co3O4 and NiO nanoparticles for photocatalytic degradation of methylene blue dye. Journal of Molecular Structure, 1143, 462-471.
[19] Varunkumar, K., Hussain, R., Hegde, G., & Ethiraj, A. S. (2017). Effect of calcination temperature on Cu doped NiO nanoparticles prepared via wet-chemical method: structural, optical and morphological studies. Materials science in semiconductor processing, 66, 149-156.
[20]- Al-Janaby, A. Z., & Al-Jumaili, H. S. (2016). Structural, optical and sensitive properties of Ag-Doped tin oxide thin films. Int Res J Eng Technol, 3(03).
[21]Fahad, O. A., Al-Jumaili, H. S., & Suhail, M. H. (2016). Studies on spray pyrolysis Sn [O. sub. 2]:[In. sub. 2][O. sub. 3] thin films for N [O. sub. 2] gas sensing application. Advances in Environmental Biology, 10(12), 89-98.
[22]- Suhail Mahdi Hasan, Al-Jumaili H.S., Abdullah Omed Gh, Characterization and NO2 gas sensing performance of CdO: In 2 O 3 polycrystalline thin films prepared by spray pyrolysis technique. SN Applied Sciences, 2019. 1(1): p. 69
[23]- Zhao, K., Gu, G., Zhang, Y., Zhang, B., Yang, F., Zhao, L., ... & Du, Z. (2018). The self-powered CO2 gas sensor based on gas discharge induced by triboelectric nanogenerator. Nano Energy, 53, 898-905.
[24] Al-Jumaili, H. S., & Jasim, M. N. (2019). Preparation And Characterization Of Zno: Sno2 Nanocomposite Thin Films On Porous Silicon As H2s Gas Sensor. Journal of Ovonic Research, 15(1), 81-87.
[25] Joshi, G., Rajput, J. K., & Purohit, L. P. (2021). SnO2–Co3O4 pores composites for CO2 gas sensing at low operating temperature. Microporous and Mesoporous Materials, 326, 111343.
[26] Molina, A., Escobar-Barrios, V., & Oliva, J. (2020). A review on hybrid and flexible CO2 gas sensors. Synthetic Metals, 270, 116602.
[27Alwan, A. M., & Dheyab, A. B. (2017). Room temperature CO2 gas sensors of AuNPs/mesoPSi hybrid structures. Applied Nanoscience, 7(7), 335-341..
[28] Grabowski, R., Słoczynski, J., Sliwa, M., Mucha, D., Socha, R. P., Lachowska, M., & Skrzypek, J. (2011). Influence of polymorphic ZrO2 phases and the silver electronic state on the activity of Ag/ZrO2 catalysts in the hydrogenation of CO2 to methanol. ACS Catalysis, 1(4), 266-278.
[29] Nasrollahzadeh, M., & Sajadi, S. M. (2015). Green synthesis of copper nanoparticles using Ginkgo biloba L. leaf extract and their catalytic activity for the Huisgen [3+ 2] cycloaddition of azides and alkynes at room temperature. Journal of colloid and interface science, 457, 141-147.

[30]- Jamal, M. S., Shahahmadi, S. A., Chelvanathan, P., Alharbi, H. F., Karim, M. R., Dar, M. A., ... & Akhtaruzzaman, M. (2019). Effects of growth temperature on the photovoltaic properties of RF sputtered undoped NiO thin films. Results in Physics, 14, 102360.
[31] Wang, X. W., Zheng, D. L., Yang, P. Z., Wang, X. E., Zhu, Q. Q., Ma, P. F., & Sun, L. Y. (2017). Preparation and electrochemical properties of NiO-Co3O4 composite as electrode materials for supercapacitors. Chemical Physics Letters, 667, 260-266..
[32]- Greenaway, D. L., & Harbeke, G. (2015). Optical Properties and Band Structure of Semiconductors: International Series of Monographs in The Science of The Solid State (Vol. 1). Elsevier..

IRAQI Academic Scientific Journals
Samarra Journal of Pure and Applied Science
SJPAS
مجلة سامراء للعلوم البحتة والتطبيقية
www.sjpas.com
p ISSN: 2663-7405
e ISSN: 2789-6838

# تحضير وتوصيف متراكب نانوي من او كسيد النيكل وأكسيد الكوبالت بواسطة طريقة الرش الحراري الكيميائي كمتحسس لغاز ثاني أكسيد الكربون

**محمد نجيب جاسم[1]*، عيد محمد مناور[2]**
قسم العلوم العامة، كلية التربية الأساسية/حديثة، جامعة الأنبار، العراق

**معلومات البحث:**
تاريخ الاستلام: 2024/07/10
تاريخ التعديل: 2024/08/17
تاريخ القبــول: 2024/09/15
تاريخ الـنشر: 2025/06/30
**الكلمات المفتاحية:**
*أوكسيد النيكل، أوكسيد الكوبلت، غاز $CO_2$، الاغشية الرقيقة متحسس الغاز*
**معلومات المؤلف**
الموبايل: 07807834988

**الخلاصة:**

تم في هذا البحث إعداد أغشية رقيقة نانوية نقية من أكسيد الكوبالت، وتم إعداد خليط من أكسيد الكوبالت ($Co_3O_4$) وأكسيد النيكل (NiO) بنسب حجمية من أكسيد النيكل تتضمن (10٪، 20٪) بطريقة الرش الكيميائي الحراري، وترسب على قواعد من الزجاج عند درجة حرارة (250 درجة مئوية). أظهرت نتائج الفحوصات بالأشعة السينية للأغشية المحضرة أنها تتكون من تركيبات متعددة البلورات، وأن الأغشية المحضرة تشكل متراكب نانوي من الكوبالت والنيكل. تم استخدام صيغة ديباي شيرر لحساب حجم البلورة. تناقصت النانومترات مع زيادة نسبة الخلط من أكسيد النيكل للأغشية المرسبة على قواعد الزجاج، حيث انخفضت من (19.6 نانومتر) لأكسيد الكوبالت النقي إلى (8.45875 نانومتر) لأكسيد الكوبالت المختلط بنسبة 20٪ نيكل. استخدم الميكروسكوب الذري (AFM) لتحديد حجم الحبيبات، ومعدل الخشونة، وجذر متوسط التربيعي للمربعات. أظهرت الصور أن سطح الأغشية متجانس، وأن الحجم الحبيبي المتوسط لجميع الأغشية هو حجم نانو وتتغير قيمته مع تغيير نسبة الخلط. تم حساب نفاذية الضوء للأغشية المحضرة باستخدام مطياف الضوء، وبالأطوال الموجية بين (1100 نانومتر إلى 3000 نانومتر). ووجد أن زيادة نسبة الخلط تؤدي إلى انخفاض في النفاذية، بينما انخفضت فجوة الطاقة البصرية أيضًا مع زيادة نسبة الخلط. أكدت النتائج أن أغشية أكسيد الكوبالت الممزوجة بأكسيد النيكل لديها درجة عالية من الحساسية تجاه غاز ثاني أكسيد الكربون، حيث تعتمد قيم الحساسية على نسب الخلط ودرجة الحرارة القاعدية وتركيز الغاز. وتم العثور على أن قيم الحساسية النسبية (S٪) لأغشية $Co_3O_4$-NiO المودعة على قواعد الزجاج تجاه غاز ($CO_2$) تصل إلى قيمة حساسية تصل إلى (70.7) في أعلى تركيز (242 جزء في المليون) وعند درجة حرارة (100 درجة مئوية)، حيث تزيد الحساسية مع زيادة تركيز الغاز. أثبتت الدراسة أيضًا أن أغشية نانوية رقيقة مختلطة من $Co_3O_4$-NiO المحضرة بطريقة التحلل الكيميائي الحراري تعطي أجهزة استشعار للغاز بخصائص جيدة تجاه ثاني أكسيد الكربون حتى عند درجة حرارة الغرفة.